Space Cryogenics Components Based on the Thermomechanical Effect: Vapor-Liquid Phase Separation

S. W. K. Yuan* and T. H. K. Frederking*
University of California, Los Angeles, California

Applications of the thermomechanical effect has been qualified including incorporation in large-scale space systems in the area of vapor-liquid phase separation (VLPS). The theory of the porous-plug phase separator is developed for the limit of a high thermal impedance of the solid-state grains. Extensions of the theory of nonlinear turbulent flow are presented based on experimental results.

Nomenclature

a_R = length in rate constant equation
A = cross-sectional area
D = diameter
f_s = VLPS factor $[1 + ST/\lambda]^{-1}$
g = gravitational acceleration
j = mass flux density (j_i with $i = n,s$)
K^* = rate constant for normal fluid convection
L = thickness of plug
L_c = characteristic length $\kappa^{1/2}$
$\dot{m}$ = mass flow rate
P = pressure
P_T = thermomechanical pressure
q = heat flux density
$\dot{Q}$ = heat flow rate
r = radial position coordinate
R = radius of tube
s = slit width
S = entropy per unit mass
t = time
T = temperature
v = velocity (v_j with $j = n,s$)
w = relative velocity ($v_n - v_s$)
z = position coordinate
η = shear viscosity
κ = permeability
λ = latent heat of vaporization
μ = chemical potential
ρ = density
ψ = wave function

Subscripts

app = apparent
d = downstream
eff = effective
n = normal fluid
o = superficial value
s = superfluid
sc = superfluid, critical
u = upstream
VLPS = vapor-liquid phase separation
ZNMF = zero net mass flow
∞ = bulk

Received Oct. 15, 1987; revision received Dec. 2, 1988.

*Lockheed Missiles and Space Company, Research and Development Division, Palo Alto, CA 94304.

I. Introduction

DEVELOPMENTS in cooling systems for space cryogenics have included utilization of the thermomechanical effect. A temperature difference may produce a pressure increase useful for pumping liquid. This effect is a peculiarity of superfluid Helium-4 below the lambda point of 2.172 K. Cooling technology has been extended into this temperature range. Uses have included the thermomechanical pressure difference for cryogen storage in a novel device called vapor-liquid phase separator (VLPS), e.g., in the large-scale telescope space vessel "IRAS" (Infrared Astronomical Satellite) flown in 1983.[1] Reliable liquid He II storage in these vessels must meet the following requirements: a small opening for vent vapor; liquid contained inside the vessel; establishment of a vapor–liquid phase boundary at a well-defined location of the phase separator; utilization of the thermomechanical pressure difference providing a retaining force against liquid escape; and a stable interface between liquid and vapor, such that the vessel's He II temperature remains constant. The pressure difference across the separator is to be kept sufficiently small, compatible with cryogenic system requirements, such as vapor-cooled shields around the vessel.

In the first proposal for a VLPS, put forward by Selzer et al.,[2] heat flows through solid separator walls. In other VLPS systems, the liquid He II carries heat; the IRAS free flyer, for instance, employs a sintered-metal porous plug made of stainless steel.

In the area of basic studies of porous media, Elsner and Klipping[3] and Elsner[4] appeared to be the first authors identifying He II equilibrium-state regimes and related phenomena. Regime classification includes "negative pressure differences" (seen from the phase-separation point of view), positive ΔP for phase separation, transition to liquid breakthrough, and "classical flow" in the breakthrough regime. In the latter, large ΔP values are significantly in excess of the thermomechanical pressure difference. Because of the focus on large flow rates in Refs. 3 and 4, few details have been resolved in the vapor–liquid phase separator regime. Subsequently, Denner et al.[5] have reported comprehensive data sets of VLPS using porous plugs. Theoretical approaches to VLPS have addressed quantification of transport in terms of the two-fluid model for He II.[6–8] Thermodynamics and two-fluid model analysis have established close relations of VLPS to "zero net mass flow" (ZNMF) heat convection.[9,11] These early efforts do lack a common frame for geometry characterization, in part due to the absence of permeability information. Comprehensive sets of plug data have been collected by Petrac for IRAS.[12] Hendricks and Karr[13] discuss a range of flow-regime possibilities based on their own data set acquisitions for VLPS plugs. Murakami[14] and Nakai and Murakami[15] have reported extensive plug measurements, pointing out that vapor flow is

possible in principle, along with two-phase flow inside the plug phase separator. Thus, surface-tension effects may play a role. Low vapor density and the accompanying continuity requirements of very high speeds and pressure differences are another consequence. Although questions regarding these limitations have remained unresolved for some time, a slit VLPS system has been adopted in theory and in experimentation.[16,17] Slit use provides a better-defined geometry than porous plug configurations. Its use is also a response to the requirement that variable flow rates accommodate different instrument dissipation rates in telescope systems. The result has been the introduction of a movable center pin inside a cylinder, an "active phase separator" (APS). A controlled flow rate as a function of time has been implemented. Klipping has undertaken a comprehensive review of the APS system.[18] A proof-of-principle experiment has shown[19] that porous media plug VLPS systems also have the capability to accommodate variable flow rates. Work in the slit device area has necessitated the introduction of an entirely different flow-regime nomenclature.

In light of the extensive variety of the VLPS device, Yuan has conducted a comprehensive experimental and theoretical investigation of VLPS plugs as part of his Ph.D. thesis.[20] The dominant effect of steady VLPS operation turned out to be *heat flow* limitations.[21,22] They appeared to be consistent with the two-fluid model rendering other effects secondary (within porous-plug data scatter). Therefore, this paper has the purpose of presenting a unifying phenomenological set of equations based on the two-fluid model of He II. Liquid convection transport is thus emphasized. The starting point is Ref. 20 and subsequent VLPS work.[23] In the latter reference, it has been possible to show that the slit device is subject to limitations similar to those of the porous plug. The apparently "linear regime" of the VLPS slit has been identified as an analog of ZNMF conditions in the *nonlinear* regime in wide ducts.[24] This finding presents encouraging possibilities for the development of basic equations in the linear regime, paralleling Ohm's law in electricity. Furthermore, the nonlinear regime is accessible, starting from permeability-related, modified ZNMF concepts. In pursuit of these goals, we begin by presenting VLPS phenomenology in Sec. II. Subsequently, in Sec. III, the two-fluid model in relation to VLPS is outlined as far as necessary for the next sections. In Sec. IV, the VLPS two-fluid kinematics equations are discussed as general results for phase separation. Section V considers linear phase-separation transport, and Sec. VI addresses nonlinear VLPS phenomena. Finally, conclusions are presented in Sec. VII.

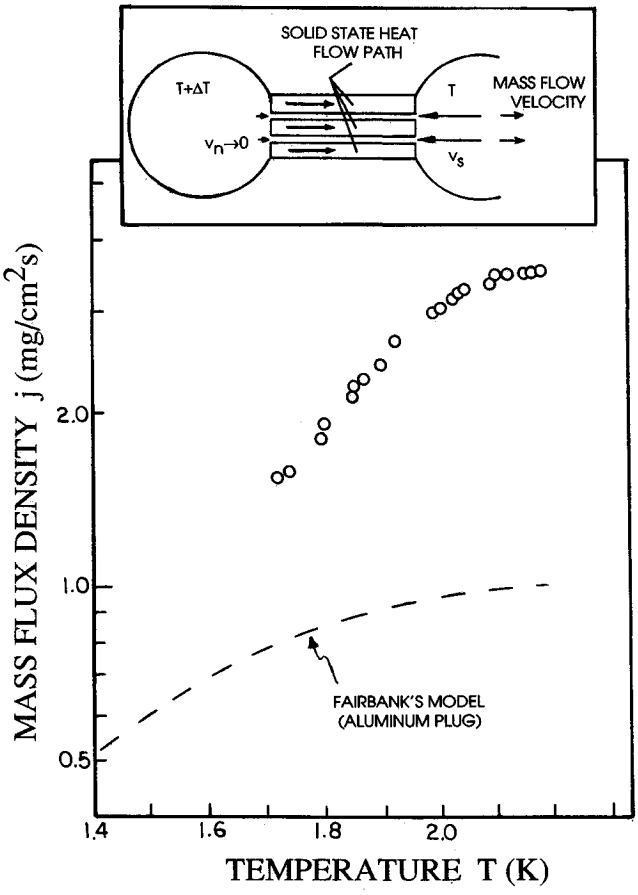

Fig. 1 Comparison of Fairbank et al. model[2] to vapor–liquid phase separation data of Klipping et al.[5] (1-μm ceramic plug).

II. He II-Vapor Phase Separation Phenomenology

Phenomena, flow modes, and various separator categories are discussed with emphasis on heat-flow conditions. There is a fluid-containing device preventing liquid escape while permitting vapor removal. This task is accomplished using the thermomechanical effect, to be quantified subsequently.

Phenomena

In the phase separator, liquid He II is converted to vapor. The heat of phase transition utilized for the phase change may flow through fluid-filled spaces, through solid components, e.g., grains of a porous medium, or through both. The heat used in the phase-separation process is supplied from the heat input into the liquid He II storage vessel. Steady states, e.g., time-independent temperatures at a separator location, require discrete flow-rate ranges for the task specified.

Flow Modes

The fluids involved in the phase-separation process may be in different flow modes. These include laminar flow, turbulent flow, and transition regimes in between. As heat may be transported through the liquid He II filling the pores of a porous plug, the theory of non-Newtonian superfluid He II is to be employed for heat-flow prediction. A most useful theoretical approach is the two-fluid model to be discussed subsequently in Sect. III.

Phase Separator System Control

Experiments have shown that appropriate sizing of the separator cross sections permits steady operation. Vapor is separated reliably from liquid He II without auxiliary means, and the vapor–liquid interface is indeed stable, as postulated in Sect. I. This type of device has been called a "passive phase separator." Passive conditions have been demonstrated primarily with porous media, such as sintered metal plugs. In addition, some specifications have included variation in flow rate for variable heat-flow rates imposed on the He II vessel, as implemented in the "active phase separator."[17]

Heat-Transport Paths

Heat may flow only through solid walls (Fairbank model of VLPS), only through liquid, or both. First, liquid He II heat-flow "path" phenomena are discussed, prior to the description of Fairbank plug properties. The inset of Fig. 1 is a schematic of the transport rate conditions.

Figure 2 presents the phase diagram $P(T)$ of He-4 with "classical" Newtonian liquid He I on the right-hand side of the lambda line, and superfluid liquid He II at the left-hand side of that phase boundary. There is no latent heat of phase change involved in the crossing of the lambda line. The isobaric specific heat is lambda-shaped, giving the phase transition its name. The need for vapor-liquid equilibrium near 1.8 K reduces the pressure at the He II-vapor phase boundary. The associated vapor pressure is near 16 mbar, i.e., approximately 1/60 of one atm. This condition is reached quite readily in space-system operation.

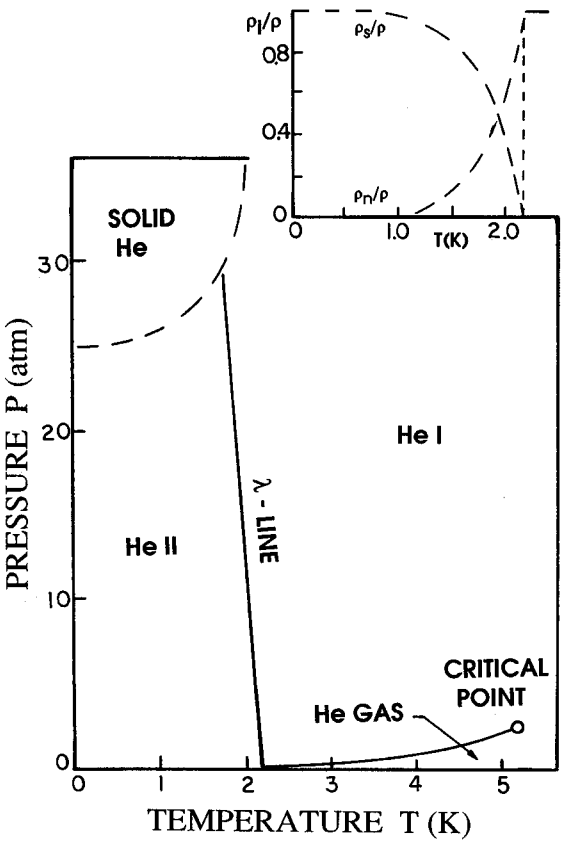

Fig. 2 Phase diagram of liquid helium; inset: density ratios vs T.

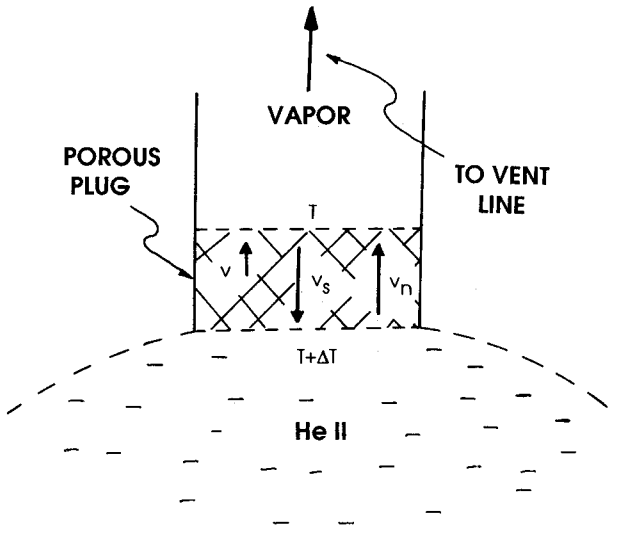

Fig. 3 Schematic diagram of vapor–liquid phase separation velocities.

Fairbank Model

This model is assessed in light of our porous-plug separator experiments and of plug results in the literature. In the ideal Fairbank separator, heat is conducted solely through solid material. A high-conductivity metal spiral, made out of aluminum, has been chosen. The heat-transport fluid of He II, called normal fluid, is clamped by viscosity in the very narrow liquid space formed. Therefore, liquid He II cannot contribute to the heat transport. The other fluid, called superfluid, is inviscid. Therefore, its density ρ_s can contribute to fluid motion. As the Fairbank model is not implemented in the present porous-plug separators, essential model results are outlined only briefly. The mass flow rate of the Fairbank model (Fig. 1) is given by the following solution:[2]

$$\dot{m} = \{\rho SL\lambda/k \pm [(\rho SL\lambda)^2/k^2 - \Delta P/A^2\rho_s]^{1/2}\}A^2\rho_s \quad (1)$$

where S and ρ are entropy and density of the liquid He II; λ is the latent heat of vaporization; ΔP is the vapor pressure difference; A and L are the cross-sectional area and thickness of the porous plug; and k is the solid-state thermal conductivity. The second term under the radical is found to be much smaller than the first. By expanding to a first-order approximation, Fairbank et al.[2] obtained

$$\dot{m} = \Delta Pk/(\rho SL\lambda) \quad (2)$$

and

$$\dot{m} = 2\rho\rho_s SLA^2\lambda/k - \Delta Pk/(\rho SL\lambda) \quad (3)$$

Equation (3) yields flow rates greatly exceeding the limit to superfluid flow called critical velocity v_{sc}. Therefore, Eq. (3) is rejected, and Eq. (2) is the physically meaningful solution of the Fairbank model.

Figure 1 presents an example which permits a comparison of Fairbank's model with porous-plug VLPS data of Denner et al.[5] (1 μm ceramic plug). The Fairbank model has been applied to an aluminum-plug system. It is seen that a bypass mechanism is operating for the low-conductivity plug[5] with relatively large pores in comparison to the Fairbank limit. This case illustrates the still-sufficiently-large transport capability of normal fluid in pores on the order of 1 μm. For a quantitative use of the two-fluid model in low-conductivity porous plugs, the various equations for superfluid and normal fluid are discussed. The inset of Fig. 1 depicts the two-fluid model velocities considered subsequently.

III. Two-Fluid Model

The basis is the postulate of well-defined "concentrations" (ρ_i/ρ, $i = s,n$). The thermodynamic equilibrium state is well defined, and concentrations are functions of T and P for bulk liquid use. The density is

$$\rho = \rho_s + \rho_n \quad (4)$$

The phase diagram depicting the He II range is shown as Fig. 2, and the inset presents the density variations with T for saturated liquid used in VLPS systems. The normal fluid is viscous with shear viscosity η_n. Since the normal fluid carries entropy, any motion of it involves heat transport. The superfluid does not have viscosity. However, resistance to flow is initiated through the creation of quantum vortices with a well-defined quantum of circulation as determined by a Bohr–Sommerfeld condition. These Onsager–Feynman vortices[25] are an important ingredient in the nonlinear transport regime of He II VLPS system. The onset of quantum vortex creation initiates at the superfluid critical velocity v_{sc}. Thus, at v_{sc} flow resistance starts to build up by vortex shedding. The mass flux densities add up to

$$\boldsymbol{j} = \rho\boldsymbol{v} = \rho_n\boldsymbol{v}_n + \rho_s\boldsymbol{v}_s \quad (5)$$

According to Landau and Lifshitz,[8] a set of simplified equations of motion is available. For the normal fluid, we have a viscous term impeding flow

$$\rho_n(\partial\boldsymbol{v}_n/\partial t) + \rho_n(\boldsymbol{v}_n \cdot \nabla)\boldsymbol{v}_n = -\rho_n/\rho\nabla P - \rho_s S\nabla T + \eta_n\nabla^2\boldsymbol{v}_n \quad (6)$$

The superfluid equation is written in terms of chemical potential $\nabla\mu$:

$$\rho_s(\partial\boldsymbol{v}_s/\partial t) + \rho_s(\boldsymbol{v}_s \cdot \nabla)\boldsymbol{v}_s = \rho_s/\rho\nabla P + \rho_s S\nabla T = \nabla\mu \quad (7)$$

The terms on the right-hand side of Eq. (6) represent a pressure gradient-related driving force contribution. This is

associated with normal fluid, a temperature gradient-related force term and the viscous force term proportional to the normal fluid shear viscosity (known in Newtonian fluid continuum description). The terms on the right-hand side of the superfluid Eq. (7) again represent the ∇P-force and the ∇T-force. Because of inviscid flow behavior, there is no viscous force impeding the superfluid. The important "nonclassical" term is the ∇T contribution called the thermomechanical effect. Consider Eq. (7) in the limit of zero velocity. Once a temperature difference has been established externally, using a fine slit (porous plug) system, then Eq. (7) predicts a thermomechanical gradient, also called "London pressure gradient" or "fountain pressure gradient," with the following condition

$$\nabla\mu = 0 \tag{8}$$

This leads to

$$\nabla P = \nabla P_T = \rho S \nabla T \tag{9}$$

Equation (7) predicts a superfluid flow as a result of a chemical potential gradient. This is readily seen by rewriting Eq. (7) in the form

$$\mathrm{D}\boldsymbol{v}_s/\mathrm{D}t = -\nabla\mu \tag{10}$$

In the VLPS mode, the superfluid motion is directed toward the interior of the He II vessel, as will be discussed in detail in Sec. IV. A low "downstream" temperature T_d is needed, seen from the mass-throughput point of view. The second law of thermodynamics requires that flow from "hot" to cold, i.e., normal fluid carrying entropy, moves in the direction of mass flow. Figure 3 shows these conditions schematically. The superfluid equation predicts flow of superfluid to establish the thermomechanical pressure gradient, Eq. (8), once a temperature gradient has been established. The steady rejection of the heat load imposed on the liquid He II vessel requires heat removal, at a rate $\dot{Q}$, proportional to the vapor mass flow rate $\dot{m}$. The thermal-energy transport rate is proportional to (ST) within the liquid. This condition requires a finite normal fluid flow velocity $\boldsymbol{v}_n$. The superfluid velocity $\boldsymbol{v}_s$ needs to match $\boldsymbol{v}_n$ according to Eq. (5).

At terrestrial gravity ("1 g"), the vessel-separator geometry (Fig. 3) is sensitive to the direction of gravitational acceleration g. Once the apparatus has been turned 180 deg, the thermomechanical pressure difference needs to be large. It must counteract the hydrostatic pressure difference in order to prevent liquid escape at 1 g. By contrast, in microgravity and under ideal conditions, only a very small thermomechanical pressure difference is needed due to the very small gravity-induced pressure difference. Ideally, therefore, only a very small temperature difference is required.

Despite these favorable conditions, the convection rates of the two fluids may be transport regime-dependent. In other words, the system of equations will permit a variety of solutions which depend on the magnitudes of velocities and on boundary conditions. One limiting case which is readily understood finds inertia effects in both fluids to be negligible. The theoretical solutions, as well as experimental results, suggest the existence of a laminar regime with linear flow response to the driving force. Prior to discussion of this linear regime (Sec. V), kinematic constraints are considered.

IV. Two-Fluid Kinematics

The phase separator discussion is focused on the liquid He II two-fluid system. This means an emphasis on porous media with low thermal conductivity grains and particle diameters on the order of magnitude of 10 μm. Evidence from the VLPS experiments[21] initially discussed suggests that *heat* convection controls the mass flow rate. This means that *normal* fluid flow limits the mass flow rate.

The kinematics of the two-fluid model provides information on the interdependence of various fluid flow rates. The following statements are considered: the definition of the relative velocity $\boldsymbol{w}$, called counterflow velocity, the general heat-flow equation, the thermodynamic vaporization equation, and the two-fluid Eqs. (6) and (7) for normal fluid and superfluid.

The counterflow velocity is

$$\boldsymbol{w} = \boldsymbol{v}_n - \boldsymbol{v}_s \tag{11}$$

The starting point for thermal transport is the invariant form of heat-transport rates of the Landau system of two-fluid equations.[6,8] The heat-flux density $\boldsymbol{q}$ involves the order parameter of the superfluid He-4, proportional to ρ_s, and the counterflow velocity

$$\boldsymbol{q} = \rho_s \boldsymbol{w} S T \tag{12}$$

The order parameter is associated with the quantum-mechanical wave function.[7] The vaporization takes place at the interfacial domain of vapor–liquid coexistence on the downstream side of the porous plug. A differential element of this domain is considered. A Euler control surface is adopted, cutting through the VLPS fluid systems on both the liquid and vapor sides, very close to the VLPS interface. The first law of thermodynamics for steady-transport results is

$$\boldsymbol{q} = j\lambda = \rho \boldsymbol{v} \lambda \tag{13}$$

The rate j is the mass-flux density, noting that mass is conserved (the enthalpy difference $\Delta H = \lambda$ is the latent heat of vaporization). The two-fluid equations are to be considered for the liquid-filled side of the VLPS plug:

$$\boldsymbol{v} = (\rho_s/\rho)\boldsymbol{v}_s + (\rho_n/\rho)\boldsymbol{v}_n \tag{14}$$

This set of six equations provides kinematic conditions established in the ideal two-fluid system. From Eqs. (5) and (12), $\boldsymbol{v}_s$ is eliminated. Using Eq. (4) in addition, one obtains $\rho_s \boldsymbol{w} = \rho(\boldsymbol{v}_n - \boldsymbol{v})$. Thus, the heat-flux density is expressed as

$$\boldsymbol{q} = ST\rho(\boldsymbol{v}_n - \boldsymbol{v}) \tag{15}$$

Eliminating $\boldsymbol{v}_n$ in Eq. (15), by means of Eq. (13), we arrive at

$$\boldsymbol{q} = \rho ST \boldsymbol{v}_n/(1 + ST/\lambda) \tag{16}$$

This result for heat-flux density of the phase-separation system is related to the heat-flux density of zero net mass flow $\boldsymbol{q}_{\mathrm{ZNMF}}$. The latter case is addressed in Appendix A because of its role as reference solution. The rate $\boldsymbol{q}$ is obtained directly from Eq. (15) for $\boldsymbol{v} = 0$:

$$\boldsymbol{q}_{\mathrm{ZNMF}} = \rho ST \boldsymbol{v}_n \tag{17}$$

Three aspects are considered in the discussion of the two-fluid kinematics: 1) the small difference between the rate $\boldsymbol{q}$ of VLPS and $\boldsymbol{q}_{\mathrm{ZNMF}}$; 2) the direction of the various two-fluid velocities; and 3) the temperature dependence of the thermophysical properties as they relate to the two-fluid kinematics.

There is only a small difference between the two heat rates of VLPS and ZNMF. The dimensionless quantity involved is the ratio of ST/λ. It reaches its largest value of 0.15 at the lambda temperature ($T_\lambda = 2{,}172$°K). As T is lowered, the ratio drops rapidly because of a steep power-law exponent $\mathrm{d}\log S/\mathrm{d}\log T \sim 5.6$. Table 1 lists various entropy values and the ratio ST/λ (compiled in Ref. 20 with entropy data based on Maynard[26]). Because of the inequality $ST \ll \lambda$ over a large T range, there is a first-order approximation of $1/(1 + ST/\lambda) \sim 1 - ST/\lambda$. Therefore, we have a simple approximation for the heat-flux density difference of

$$\boldsymbol{q}_{\mathrm{ZNMF}} - \boldsymbol{q} \sim (ST/\lambda)\boldsymbol{q}_{\mathrm{ZNMF}} \tag{18}$$

Table 1 Entropy and ratio ST/λ of saturated liquid He II at vapor-liquid equilibrium

T, K	S, J/g-K	ST/λ	$[1 + ST/\lambda]$
2.1	1.2316	0.112	0.899
2.0	0.9465	0.081	0.925
1.9	0.7228	0.059	0.944
1.8	0.5427	0.042	0.960

The telescope He II vessels are specified for a long "lifetime," available until the last droplet of liquid disappears. The task imposed is the minimization of heat input into the liquid. Equations (13) and (15) both point out the consequence of a small v required for vessel operation.

In particular, Eq. (15) relates to the frequently investigated ZNMF mode which provides considerable insights into heat-flow aspects of phase-separator operation.

The second point, the directional aspect, is considered on the basis of q vs v_s. The normal fluid velocity is eliminated from Eq. (5) using Eqs. (11) and (13). This leads to

$$j = v_s\rho + w\rho_n = q/\lambda \tag{19}$$

Furthermore, the counterflow velocity w is removed using Eq. (12). The resulting form for the heat-flux density is

$$q = -v_s\rho_s ST\phi \tag{20}$$

where ϕ is a function solely of the thermophysical properties of superfluid He II

$$\phi = 1/[(\rho_n/\rho) - (\rho_s/\rho)(ST/\lambda)] \tag{21}$$

The thermophysical property function ϕ has positive values in the T range under consideration. Therefore, Eqs. (20) and (21) predict a q direction in counterflow to the superfluid velocity v_s. The normal fluid velocity of Eq. (16) is parallel to q, in line with the second law of thermodynamics. Therefore, the counterflow conditions are quite similar to the ZNMF mode insofar as superfluid is in counterflow to normal fluid. The net mass velocity of VLPS [Eq. (13)] is seen to be parallel to the normal fluid velocity. However, its speed is quite small [Eq. (15)] in comparison with the magnitude of the normal fluid velocity.

Concerning the third aspect, the T dependence of properties, we note that Eq. (12) describes q as a function of (ρ_s/ρ), i.e., of the state of order. Order is fully established at $T = 0$ K. Any superfluid order is lost ($\rho_s = 0$) at the "high"-T limit, the lambda temperature. Therefore, Eq. (12) predicts a breakdown of the present VLPS result. This could also be seen as the disappearance of an efficient thermomechanical pressure difference availability for phase separation at the lambda point.

V. Linear Phase-Separation Transport

Local kinematic conditions have been addressed until this point. For zero net mass flow (Appendix A), however, there is only a matching of *mean velocities* ($|\rho_s v_s| = |-\rho_n v_n|$). Similarly, we expect that mean velocities ought to agree with the preceding two-fluid kinematics equations. No detailed experimental probing of the local ZNMF velocities in very small pores appears to have been reported. In fact, conventional porous-media equations make use of mean approach velocities ("superficial velocities") for the plug. Therefore, transport in the linear phase-separation regime is quantified using the corresponding approach velocities for the two-fluid system. First, the theoretical results of the laminar regime of negligible inertia are summarized. Subsequently, experimental results are considered.

VLPS Transport Equations at Negligible Inertia

For Newtonian fluids, the "classical" low-speed version of flow through porous media is Darcy's law (subscript zero indicating approach velocities)

$$v_0 = \kappa|\nabla P|/\eta \tag{22}$$

The normal fluid behaves as a special Newtonian fluid subject to the thermomechanics of superfluid He II. Therefore, the analog of Darcy's law for normal fluid is found to rely readily on the procedures for ZNMF (Appendix A). The ZNMF approach velocity of normal fluid flow is

$$v_{n0} = \kappa_n|\nabla P|/\eta_n \tag{23}$$

The related ZNMF heat-flux density has the approach value

$$q_{\text{ZNMF}} = \rho ST v_{n0} \tag{24}$$

Referring to the major two-fluid kinematics results for phase separation, Eq. (16), we rewrite q for VLPS as approach heat-flux density

$$q_0 = q_{\text{ZNMF}}/(1 + ST/\lambda) \tag{25}$$

Introducing an axial position coordinate z, along the axis of fluid-carrying device, we combine Eqs. (23), (24), and (9) to get

$$q \cdot dz = \kappa_n \rho ST\, dP_T/\eta_n \tag{26a}$$

or

$$q \cdot dz = (\rho^2 S^2 T\, dT/\eta_n)\kappa_n \tag{26b}$$

Integration of Eq. (26), subject to an initial bath temperature in terms of mass flow rate $\dot{m}$ [Eq. (13)], results in

$$\dot{m}/A = j = (\kappa_n/L)\int_{T_d}^{T_u} (\lambda + ST)^{-1}[\rho^2 S^2 T\, dT/\eta_n] \tag{26c}$$

Figure 4 is a plot of Eq. (26c) with $(\kappa_n/L) = 10^{-7}$ cm.

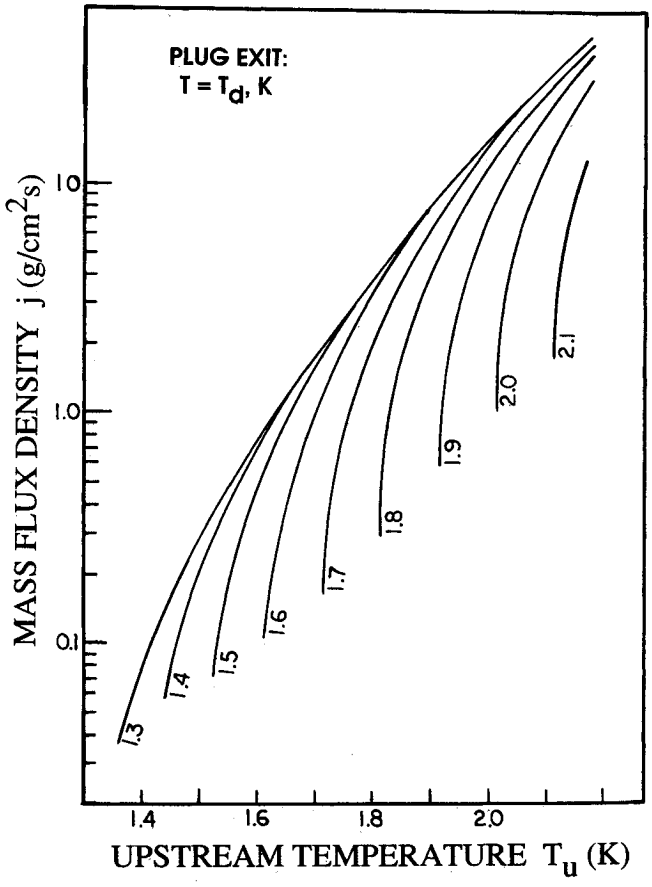

Fig. 4 Laminar mass flow density for a finite temperature difference, as the upstream temperature is varied; parameter: downstream temperature T_d.

Experimental Linear Regime Data

The scarce data sets appear to be among the reasons for limited recognition of Eq. (26c). Although the close relationship between ZNMF and VLPS [Eq. (25)] has been observed early,[11] the controlling role of heat/normal fluid transport has been recognized only partially.[16] In principle, permeabilities of Eqs. (22) and (23) may be generalized to include ducts (with vanishing wall thickness). The following permeability values describe a slit of width s, and a capillary of diameter D:

Very narrow slit: $\kappa_n = s^2/12$

Capillary: $\kappa_n = D^2/32$

The necessary requirement is fully developed flow. In this area, the work of Murakami[14] indicates, in part, laminar flow while adopting a modified phenomenological equation. Hendricks and Karr[13] also report linear-regime data.

Figures 5 and 6 present comparisons of VLPS and ZNMF. Figure 5 is a plot of κ_n data for VLPS with a 1-μm ceramic porous plug.[5] Figure 6 shows apparent $(\kappa_n)_{app}$ values of the ZNMF mode (2-μm stainless steel plug). Only at low temperatures do the data indeed support the linear equations as far as the temperature dependence is concerned. If the linear-regime transport rates, expressed as permeabilities, are indeed meaningful, there ought to be only slight departures of VLPS data from ZNMF data. In principle, well-defined media with repetitive grain-pore domains permit calculation of permeabilities from first principles. However, sintered-plug products of manufacturing lines, used in the present work, do not show ideal repetitive geometry. Therefore, the experimental determination of permeabilities is more reliable, e.g., measurements of the room-temperature Darcy value [Eq. (22)], or ZNMF determination of κ_n from heat-flow runs in He II [Eq. (23)].

The data of Fig. 5 suggest a low-temperature κ_n value of 10^{-11} cm^2. The results of Fig. 6 show a κ_n of 2×10^{-9} cm^2. The data trends at "high-T," in both figures, suggest a reduced apparent permeability $(\kappa_n)_{app}$. This behavior has been recognized qualitatively for ZNMF as the result of mutual friction phenomena.[27] The nonlinear regime modeling in the next section aims at a resolution of the additional flow resistance in terms of porous-media permeabilities and thermophysical properties.

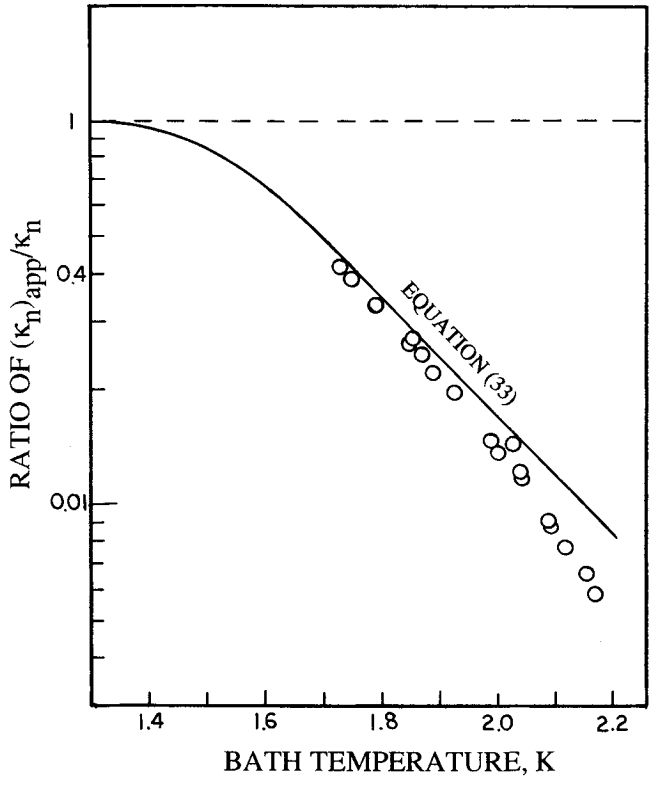

Fig. 5 Apparent normal fluid permeability of VLPS data tending toward a constant Darcy value at low T.[5]

VI. Nonlinear VLPS Regime

The kinematic equations of Sec. IV show that the VLPS heat-convection rate, established by normal fluid flow, is close to the VLPS rate (compared to porous-plug data scatter). There is no specific reference to the *mode* of normal fluid flow. Therefore, it appears to be meaningful to retain the factor $[1 + ST/\lambda]^{-1}$ also in the nonlinear regime. In addition, ZNMF experience (reviewed by Tough[28]) ought to be useful for the development of phenomenological equations in the nonlinear regime.

Above the critical rate of normal fluid flow, ZNMF results for *wide* ducts suggest that the "apparent normal fluid permeability" decreases upon an increase in q. There is a dissipative term, called "mutual friction," involving superfluid and normal fluid interaction. Onsager–Feynman quantum vortices[25] are created from the superfluid (whose low energy state has zero entropy). The entropy-carrying vortices modify the normal fluid flow phenomena (at "supercritical" normal fluid velocities) in a manner similar to the action of vorticity of turbulent eddies in "classical" Newtonian fluid flow. More precisely, there is an asymptotic limit of large ΔT characterized by d log q/d log $D = 0$ ("chaos limit"). This limit is associated with the original investigations of Gorter and Mellink[27] concerning mutual friction. The wide-duct phenomena have been characterized by a rewritten "mutual-friction equation," rewritten for chaos in terms of similitude conditions, with one single constant and a function involving thermophysical properties.[24] It has been known for some time that the transition from linear flow to chaos is quite complex, as shown by Tough[28] for ZNMF. The recent nonlinear VLPS regime of the *slit* device has been described[23] by an analog of the mutual-friction chaos equation taking into account the VLPS (entropy/latent heat) factor, $f_s = [1 + ST/\lambda]^{-1}$. The equation for a differential in temperature is

$$q_0 = \rho_s ST w_{eff}/[1 + ST/\lambda] \tag{27}$$

with

$$w_{eff} = K_\infty [(\rho_s/\rho_n) S(dT/dz)\eta_n/\rho]^{1/3} \tag{28}$$

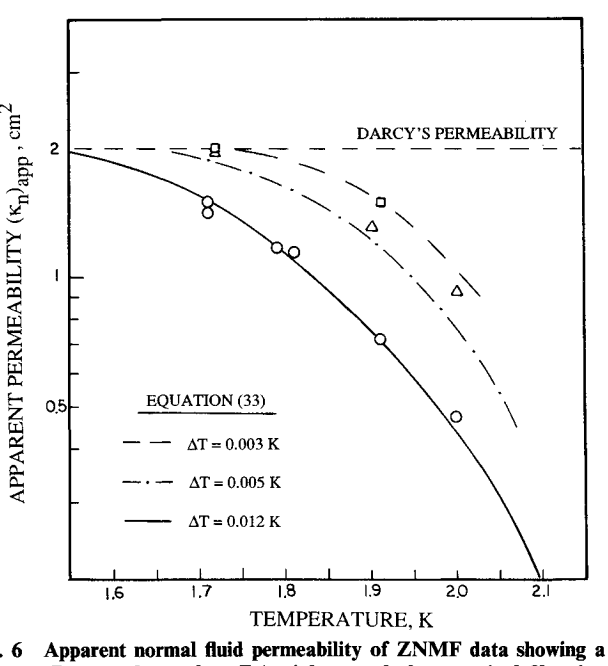

Fig. 6 Apparent normal fluid permeability of ZNMF data showing a constant Darcy value at low T (stainless steel plug, nominal filtration rating 2 μm, PSM).

The constant for APS has been found[23] to be $K_\infty = 10$, close to the ZNMF value of 11.3 of Ref. 24. For the most part, the chaos equation involves a large temperature difference. Therefore, it is necessary to integrate the equation assuming steady flow. The integration is accomplished readily as variables are separated easily. For instance, q_0 is obtained for heating the vessel's He II to $(T_d + \Delta T)$ as

$$q_0 = K_\infty L^{-1/3}\left\{\int_{T_d}^{T_d+\Delta T} [1 + ST/\lambda]^{-3} \times (\rho_s ST)^3 S(\rho_s/\rho_n)(\eta_n/\rho)\, dT\right\}^{1/3} \quad (29)$$

(where $T_u = T_d + \Delta T$). The related mass-flux density j_0 (=mass flow rate $\dot{m}$ divided by the total plug cross section) is

$$j_0 = q_0/\lambda \quad (30)$$

It has been recognized for a considerable time that mutual friction in porous media and fine ducts is altered significantly, in particular for fine pores.[29] For this reason, the VLPS porous-plug flow rates are not predicted in a straightforward manner. Therefore, the complex VLPS turbulence forces a reliance on semiempirical use of experimental data.[20] It turns out that for each plug there is a particular plug constant, the nonlinear rate constant K^*. Thus, the value K_∞ for the *wide* slit system [Eqs. (27) and (28)] is replaced by the pore-size-dependent constant K^*.

VLPS plug transport, expressed as mass-flux density escaping at the plug exit, is quantified by the following result:

$$j_0 = K^* L^{-1/3}\left\{\int_{T_d}^{T_d+\Delta T} [\lambda + ST]^{-3} \times (\rho_s ST)^3 S(\rho_s/\rho_n)(\eta_n/\rho)\, dT\right\}^{1/3} \quad (31)$$

A similar result for T_d reduction at the vent side involves the integral from $(T_u - \Delta T)$ to T_u in the vessel. The thermophysical property exerting the most distinct temperature influence is the entropy S. The product S^4T is proportional to $T^{23.4}$. As the vessel temperature approaches the lambda point, the superfluids density drops sharply. The factor ρ_s^3 under the integral produces a leveling off in the mass flow rates in Fig. 7 above about 2 K. Similarly, in Fig. 8, there is a pronounced leveling of the rates at low temperatures. The dimensionless rate constants have been determined from He II VLPS experiments, and permeability has been obtained by a suitable technique. The VLPS plug data are described, to first order and within data scatter, by the following dimensionless VLPS rate constant:

$$K^* = L_c/a_R \quad (32)$$

The range covered is for nominal pore sizes from the order of 0.5 to 10 μm. This corresponds to characteristic length $L_c = (\kappa_n)^{1/2}$ below 10 μm down to the order of magnitude 0.1 μm. The reference length in Eq. (32) is $a_R \sim (10^{-7})^{1/2}$ cm. It is observed that the permeability of ductile plug materials, such as stainless steel, does not decrease significantly upon cooldown to 1.8 K (unless severe stress changes the geometry). Therefore, Eq. (31) suggests that the ratio j_0/K^* ought to be a unique function of temperature difference for a specified plug end temperature. Results are summarized in the two parts of Fig. 9. Figure 9a describes data for decreasing downstream temperature T_d as the vessel's bath temperature T_u is kept constant. Figure 9b presents results for different ΔT as the vent temperature T_d at the plug exit (=liquid He II saturation temperature) is kept constant and T_u is raised.

In addition, it is useful to quantify the apparent permeability, at least to first order. The manufacturer's sintered products are characterized by a finite grain size and pore-size distribution. This behavior masks many details of the flow

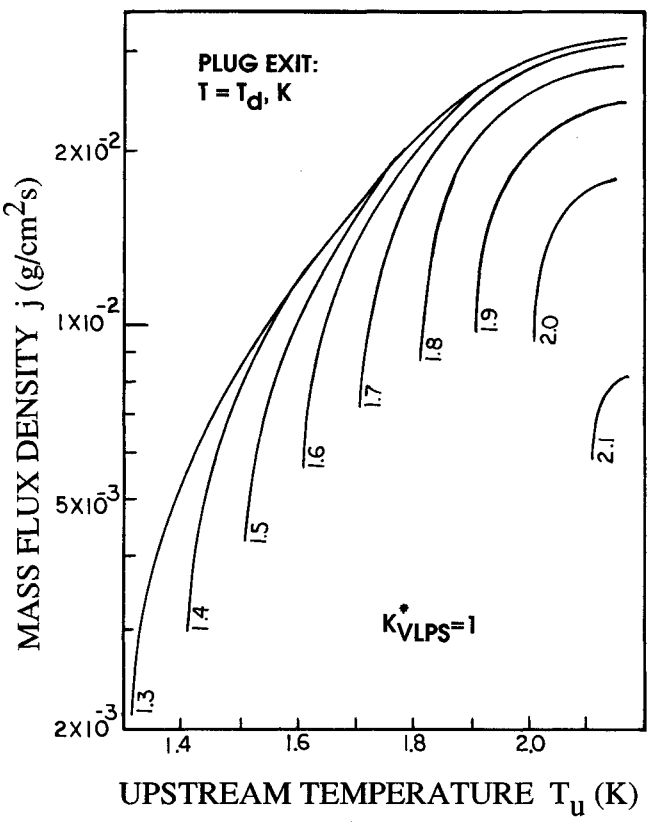

Fig. 7 Nonlinear flow conditions: mass-flux density of Eq. (31) for a constant downstream temperature while the upstream temperature is varied.

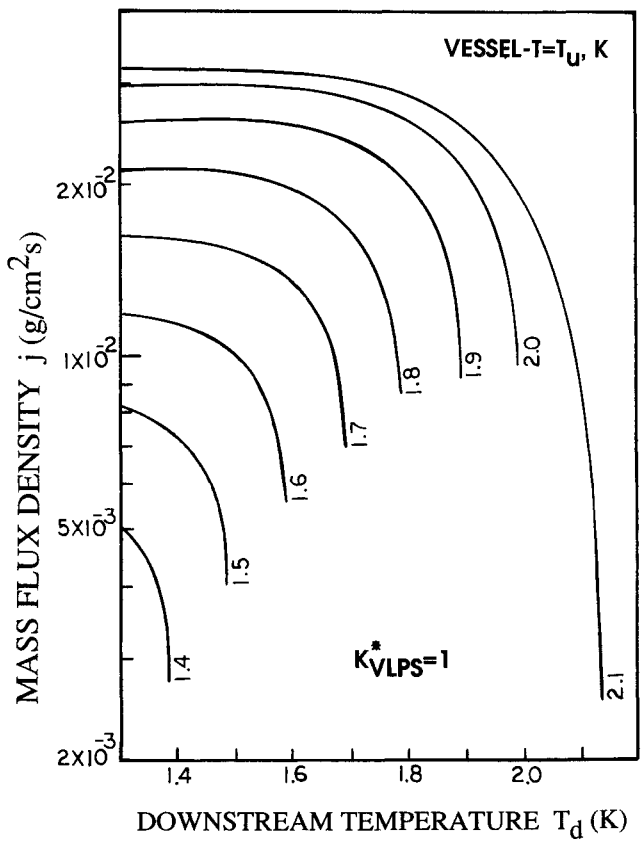

Fig. 8 Nonlinear flow conditions: mass-flux density of Eq. (31) for a constant bath temperature $T = T_u$ while the downstream temperature is varied.

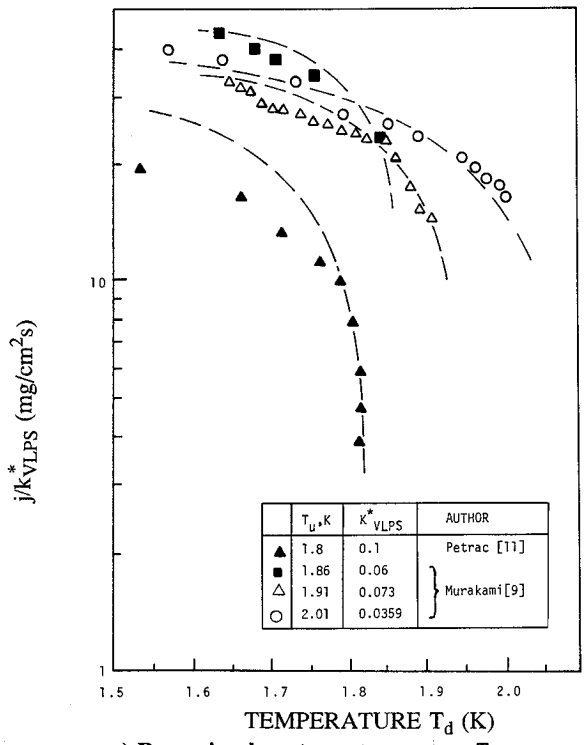

a) Decreasing downstream temperature T_d

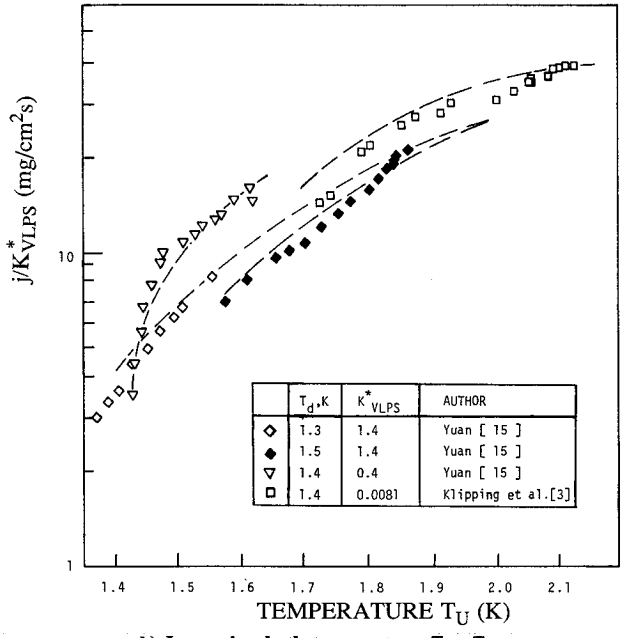

b) Increasing bath temperature $T = T_u$

Fig. 9 Summary of various phase-separator results (Refs. 20–22) given as ratio j_0/K^*.

transition process, observed for instance in wide ducts at ZNMF. This creates a gradual transition from the linear flow regime of normal fluid convection to the nonlinear regime. Derivation of this interpolation equation for apparent permeability is presented in Appendix B. The result is an integral expression. A suitable phenomenological equation for the VLPS range covered ought to be similar to the ZNMF flow case. The VLPS equation for the apparent permeability is

$$(\kappa_n)_{\text{app}} = \kappa_n[1 + F_T(\Delta T, T)]^{-1/3} \tag{33}$$

with

$$F_T \propto \Delta T^2 \tag{34}$$

The ZNMF equation corresponding to the VLPS equation is readily obtained using $f_s = 1$. Equation (33) has been included in Figs. 5 and 6. It is seen that there is excellent agreement between the equation and the data.

VII. Conclusions

The following conclusions are drawn concerning the present VLPS plug work.

1) The linear regime is described by a simple law resembling "Ohm's law." The rate-controlling normal fluid approach velocity is proportional to the London pressure gradient, to the normal fluid permeability, and to the reciprocal shear viscosity of normal fluid.

2) The nonlinear regime is described, to first order, and within data scatter, by the "chaos" related rate constant K^* for the regime of size-independent heat-flux densities, i.e., relatively wide pores.

3) An interpolation equation describing a smooth transition between the linear regime and the nonlinear regime is useful for the apparent permeability ratio (see Appendix B also).

The consequences of porous-media employment are outlined as far as sizing of VLPS plugs is concerned. A low-temperature run is useful for the determination of the normal fluid permeability (in verification of manufacturer information for room temperature). It is convenient to check the nonlinear "chaos" rate constant near the transition in a low-temperature run.

It is noted that for the order of a heat-rejection rate at 10 mW, the mass flow rate of the VLPS plug is on the order of 1 mg/s. Thus, after adoption of a plug product of a given cross section to thickness ratio, the equations presented allow dimensioning of the VLPS plug. (See Appendix C for a design example.)

Appendix A: Zero Net Mass Flow (ZNMF) in the Linear Regime

Consider Eq. (5) for the special case of zero net flow $\boldsymbol{j} = 0$. The superfluid rate of flow (per unit area and time) is directly related to the normal fluid rate:

$$\rho_s \boldsymbol{v}_s = -\rho_n \boldsymbol{v}_n \tag{A.1}$$

Normal Fluid

Negligible inertia forces in Eqs. (6) and (7) lead to a simple statement. The truncated equations are added subject to Eq. (4). The resulting differential equation is

$$0 = -\nabla P_T + \eta_n \nabla^2 \boldsymbol{v}_n \tag{A.2}$$

Differential Eq. (A.2) is an analog of a Newtonian fluid flowfield description, subject to Newtonian immobilization of normal fluid at impervious walls, i.e., adiabatic boundary conditions noting Eq. (15). Thus, in principle, known solutions for Stokes flow or Navier-Darcy flow may be modified in order to describe thermal energy convection in liquid He II. The mean velocity of normal fluid flow may be expressed in terms of a generalized Darcy law as

$$\boldsymbol{v}_n = \kappa_n |\nabla P_T| / \eta_n \tag{A.3}$$

Superfluid

The Ginzburg–Landau equations include solutions for uniform flow of superfluid. The differential equations are written in terms of the wave function ψ. [An analog for heat flow (not superflow) turned out to be not directly verified by experimental data.] The resulting solution expresses the lowering of the order parameter due to a finite kinetic energy of flow (flow power). The uniform flow terminates at a wall distance on the order of the de Brodlie wavelength (coherence length). As long as order is established well, i.e., for reasonable ρ_s values

(Fig. 2, inset), the uniform flow appears as "plug flow" to the macroscopic observer. It is convenient to compare the parabolic v distribution to the flat superfluid profile. For instance, the normal fluid velocity in a tube with adiabatic walls is

$$v_n = (v_n)_{\max}[1 - (r/R)^2] \tag{A.4}$$

It is concluded that ZNMF is violated *locally*, but it may be maintained readily *globally*, as mean speed criterion, up to critical conditions for onset of nonlinear effects.

Appendix B: Apparent Darcy's Permeability

The transition between linear and nonlinear heat transport in porous media can be described by the following interpolation equation:[20]

$$1/q = \left[\sum (1/q)^3\right]^{1/3} = [(1/q_{\text{LIN}})^3 + (1/q_{\text{NL}})^3]^{1/3} \tag{B.1}$$

where q_{LIN} and q_{NL} are the linear and nonlinear terms, respectively. Rearranging the above equation one gets

$$q/q_{\text{LIN}} = 1/[1 + (q_{\text{LIN}}/q_{\text{NL}})^2]^{1/3} \tag{B.2}$$

Substituting $q = (\kappa_n)_{\text{app}} \rho S T \nabla P_T/\eta_n$ and Eq. (24) for q_{LIN}, Eq. (B.2) becomes

$$(\kappa_n)_{\text{app}}/\kappa_n = 1/[1 + (q_{\text{LIN}}/q_{\text{NL}})^3]^{1/3} \tag{B.3}$$

Inserting Eqs. (13) and (26c) for q_{LIN} and Eq. (31) for q_{NL}, respectively, one obtains

$$(\kappa_n)_{\text{app}}/\kappa_n = 1/[1 + F(T)]^{1/3}$$

where

$$F(T) = \kappa_n^3(\rho_n/\rho)(S\Delta T/L)^2/K^{*3}[(\rho_s/\rho)(\eta_n/\rho)]^4$$

$$\Delta T \ll T \tag{B.4}$$

The above equations (or Eqs. 33 and 34) are used to calculate the apparent permeability in Figs. 5 and 6.

Appendix C: Design Example

For a heat-rejection rate of 100 mW, the boil-off rate required to maintain a constant bath temperature (by the removal of latent heat) is

$$\dot{m} = q/\lambda = 100(\text{mW})/20(\text{J/g-K}) \sim 5\ \text{mg/s} \tag{C.1}$$

Note that $\dot{m} = j_0 A$, and Eq. (31) can be written as

$$\dot{m} = K^*(A/L^{1/3})\left\{\int_{T_d}^{T_d+\Delta T} (\rho_s ST/\lambda + ST)^3 \times S(\rho_s/\rho_n)(\eta_n/\rho)\, dT\right\}^{1/3} \tag{C.2}$$

For a bath temperature of 1.8 K and a ΔT of the order of 100 mK, one can estimate the dimension of the porous plug $(A/L^{1/3})$. Assuming a 0.5-μm Mott porous plug with a permeability of 8×10^{-10} cm^2, the rate constant K^* can be obtained from Eq. (32) to be $\sim$0.09. From Eq. (C.2), the plug product $(A/L^{1/3})$ is calculated to be about 3, which is in good agreement with the experimentally determined value of the in-flight IRAS phase-separator plug.[30]

Acknowledgments

The partial support of this work by NASA Ames Research Center is acknowledged with appreciation. Various collaborators of the present laboratory (UCLA) have also contributed.

References

[1]Urbach, A. R. and Mason, P. V., "IRAS Cryogenic Flight System Flight Performance Report," *Advances in Cryogenic Engineering*, Vol. 29, Plenum Press, New York, 1984, pp. 651–659.

[2]Selzer, P. M., Fairbank, W. M., and Everett, C. W. F., "A Superfluid Plug for Space," *Advances in Cryogenic Engineering*, Vol. 16, Plenum Press, New York, 1971, pp. 277–281.

[3]Elsner, A. and Klipping, G., "Control System for Temperatures and Liquid Level Between 4.2°K and 1°K," *Advances in Cryogenic Engineering*, Plenum Press, New York, Vol. 14, 1969, pp. 416–422.

[4]Elsner, A., "Flow of Helium Through Very Fine Filters," Ph.D. Thesis, Free Univ., Berlin, 1969.

[5]Denner, H. D., Klipping, G., Klipping, I., Menzel, J., and Rupert, U., "Flow of Helium Through Porous Plugs," *Cryogenics*, Vol. 18, 1978, pp. 166–170.

[6]Khalatnikov, I. M., *Introduction to the Theory of Superfluid*, Benjamin, New York, 1965, Pt. II, pp. 55–62.

[7]Ginsburg, V. L. and Pitaevskii, L. P., "On the Theory of Superfluidity," *Soviet Physics JETP*, Vol. 34, 1958, pp. 858–861.

[8]Landau, L. D. and Lifshitz, E. M., *Fluid Mechanics*, Pergamon, London, 1959, pp. 507–522.

[9]Caspi, L., Lee, J. Y., and Frederking, T. H. K., "Lambda Transition (He II–He I) During Heat Flow at Supercritical Pressures," *Journal of Heat Transfer*, Vol. 99, 1977, pp. 479–482.

[10]Kamioka, Y., "The Prediction of Steady-State Heat Flux and Related Temperature Profiles in Pressurized Superfluid Helium II," *Cryogenics*, Vol. 23, 1983, pp. 367–372.

[11]Chuang, C., Kim, Y. I., and Frederking, T. H. K., "Vapor–Liquid Phase Separation of Cryogenic Liquid Storage Systems Below the Lambda Point (He^4)," *Cryogenic Processing Equipment*, American Society of Mechanical Engineers, Publication No. H 00164, New York, 1980.

[12]Petrac, D., "Development Tests and Analysis Performed at JPL," JPL Rept., July–Sept. 1979.

[13]Hendricks, J. B. and Karr, G. R., "Operation of Phase Separators in Zero Gravity," *Cryogenics*, Vol. 27, 1987, pp. 49–53.

[14]Murakami, M., "Thermo/Fluid Dynamics of He II Flow Through Porous Media," *Proceedings of the Space Cryogenic Workshop*, Berlin, FRG, 1984, pp. 70–82.

[15]Nakai, H. and Murakami, M., "Flow Phenomena of Superfluid Helium Through a Porous-Plug Phase Separator," *Cryogenics*, Vol. 27, 1987, pp. 442–449.

[16]Schotte, U. and Denner, H. D., "Heat Conduction Through Narrow Channels and Phase Separation of He II at Zero Gravity," *Zeitschrift fuer Physik B*, Vol. 41, 1981, pp. 137–145.

[17]Denner, H. D., Klipping, I., Lunders, K., Menzel, J., and Ruppert, U., "The Evaporation of He II Through Narrow Channels," *Proceedings of the Seventh International Cryogenic Engineering Conference*, London, England, 1978, pp. 240–244.

[18]Klipping, G., "Scientific and Engineering Aspects of the Active Phase Separator," *Advances in Cryogenic Engineering*, Vol. 31, Plenum Press, New York, 1986, pp. 851–860.

[19]Frederking, T. H. K., Chuang, C., Kamioka, Y., Lee, J. M., and Yuan, S. W. K., "Sintered-Plug Flow Modulation of a Vapor–Liquid Phase Separator for a Helium II Vessel," *Advances in Cryogenic Engineering*, Vol. 29, Plenum Press, New York, pp. 687–695.

[20]Yuan, S. W. K., Ph.D. Thesis, Univ. of California, Los Angeles, CA, 1985.

[21]Yuan, S. W. K. and Frederking, T. H. K., "Heat and Mass Transfer in Porous Media Phase Separation Below the Lambda Point of Helium-4," *Heat Transfer 1986, Proceedings of the 8th International Heat Transfer Conference*, Hemisphere Publishing, Washington, D.C., Vol. 5, pp. 2683–2686.

[22]Yuan, S. W. K. and Frederking, T. H. K., "Nonlinear Vapour-Liquid Phase Separation Including Microgravity Effects," *Cryogenics*, Vol. 27, 1987, pp. 27–33.

[23]Yuan, S. W. K., Lee, J. M., and Frederking, T. H. K., "Turbulent Transport of He II in Active and Passive Phase Separators Using Slit Devices and Porous Media," *Advances in Cryogenic Engineering*, Vol. 33, Plenum Press, New York, 1987, pp. 431–439.

[24]Soloski, S. C. and Frederking, T. H. K., "Dimensional Analysis and Equation for Axial Heat Flow of Gorter-Mellink Convection (He II)," *International Journal of Heat and Mass Transfer*, Vol. 23, 1980, pp. 437–441.

[25]Feynman, R. P., "Application of Quantum Mechanics to Liquid Helium," *Progress in Low-Temperature Physics*, Vol. 1, North Holland Publishing, Amsterdam, 1955, pp. 17–53.

[26]Maynard, J., "Determination of the Thermodynamics of He II from Sound-Velocity Data," *Physics Reviews*, Vol. 14, 1976, pp. 3868–3890.

[27]Gorter, C. J. and Mellink, J. H., "On the Irreversible Processes in Liquid He II," *Physica*, Vol. 15, 1949, pp. 285–304.
[28]Tough, J. T., "Superfluid Turbulence," *Progress in Low-Temperature Physics*, edited by D. F. Brewer, North Holland Publishing, Amsterdam, 1982, pp. 133–219.
[29]Hammel, E. F. and Keller, W. F., "Narrow Channel Flow," *Superfluid Helium*, edited by J. F. Allen, Academic Press, New York, 1966, pp. 121–146.
[30]Petrac, D. and Mason, P. V., "Infrared Astronomical Satellite (IRAS) Superfluid Helium Tank Temperature Control," *Proceedings of 1983 Space Helium Dewar Conference*, University of Alabama, Huntsville, AL, pp. 163–169.